

Phase Behavior of a Sodium Dodecanol Allyl Sulfosuccinic Diester/*n*-Pentanol/Methyl Acrylate/Butyl Acrylate/Water Microemulsion System and Preparation of Acrylate Latexes by Microemulsion Polymerization

Aixi Hu,¹ Zhigang Yao,² Xi Yu²

¹College of Chemistry and Chemical Engineering, Hunan University, Changsha, Hunan 410082, People's Republic of China

²College of Chemistry and Chemical Engineering, South China University of Technology, Guangzhou, Guangdong 510640, People's Republic of China

Received 29 February 2008; accepted 4 January 2009

DOI 10.1002/app.30284

Published online 27 April 2009 in Wiley InterScience (www.interscience.wiley.com).

ABSTRACT: Pseudoternary phase diagrams of quaternary microemulsion systems composed of the reactive surfactant sodium dodecanol allyl sulfosuccinic diester, *n*-pentanol, methyl acrylate/butyl acrylate, and water were made. The influence of the mass ratio of sodium dodecanol allyl sulfosuccinic diester to the cosurfactant (*n*-pentanol) in the system and the influence of electrolyte sodium chloride on the microemulsion area were examined. The microstructure of the microemulsion was determined with a conductance technique. The results suggested that there were three structures in the microemulsion system: water in oil, oil in water, and a bicontinuous phase. Microemulsion polymerizations were carried with some point in the microemulsion region being chosen as the formulation. The structure and

configuration of the polymer latexes were determined and analyzed with Fourier transform infrared, differential scanning calorimetry, and scanning electron microscopy. The results suggested that the reactive surfactant could participate in the polymerization with the monomers to some extent; the glass-transition temperature of the latex was -31.4°C . The polymer latex was transformed gradually from an open porous structure to a closed porous structure when its pregnant microemulsion was varied from a bicontinuous structure to an oil-in-water structure. © 2009 Wiley Periodicals, Inc. *J Appl Polym Sci* 113: 2202–2208, 2009

Key words: emulsion polymerization; phase behavior; surfactants; synthesis

INTRODUCTION

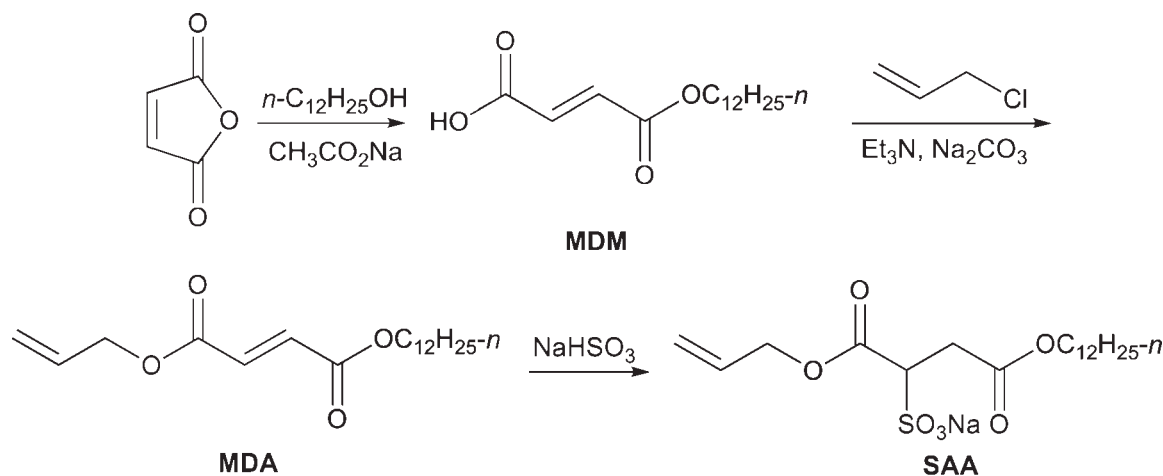
Reactive surfactants are new surfactants containing reactive groups. They can assemble spontaneously to form microemulsions.¹ Unsaturated bonds in microemulsions may lead to a polymerization reaction initiated by light or heat, so the microemulsions can maintain their original aggregation state and have higher stability. These merits of microemulsions offer some potential for the preparation of organic materials.^{2–4} They can also be applied to inorganic materials^{5,6} and biological pharmaceuticals⁷ as various chemical-reactive media. In microemulsion polymerization, using a reactive surfactant as an emulsifier effectively prevents two-phase separation and keeps the whole system in the microemulsion state for polymerization. Moreover, a reactive surfac-

tant can participate in the polymerization reaction more advantageously under this condition. Because reactive surfactants provide particular and better performance, many polymers with specific structures are synthesized through microemulsion polymerization. These polymers have many merits, including small apertures and manageable aperture states and structures, so they can form lots of macromolecular polymers such as open porous latexes, high-oil-absorption resins, and waterproof coatings and can be applied widely in various areas. However, the matrix microemulsions used for microemulsion polymerization come into being only in the range of a definite formula ratio. In addition, the microemulsion structure obviously influences the stability of microemulsions and the performances of polymers. Therefore, it makes sense to study the phase behavior of polymerization systems. There have been few systems for correlative research so far,^{8–15} and studies on the phase behavior of microemulsions using reactive surfactants have not been reported in detail.

In this study, a homemade reactive surfactant, sodium dodecanol allyl sulfosuccinic diester (SAA), was used in a microemulsion, and the phase

Correspondence to: A. Hu (axhu0731@yahoo.com.cn).

Contract grant sponsor: Scientific Research Fund of the Hunan Provincial Education Department; contract grant number: 04B058.



Scheme 1

behavior of an SAA/*n*-pentanol/methyl acrylate (MA)/butyl acrylate (BA)/water microemulsion system was studied. Pseudoternary phase diagrams of the quaternary microemulsion systems were made, the variational rule of conductivity following the water ratio was observed, and the microemulsion microstructure was confirmed. Subsequently, microemulsion polymerization was carried out to prepare latexes of different configurations; meanwhile, the structures and performances of the latexes were examined. This is a significant study, offering some theoretical guidance for the exploitation and application of this reactive surfactant.

EXPERIMENTAL

Materials

Unless stated otherwise, all reagents and chemicals were obtained commercially and used without further purification. Maleic anhydride was purchased from Tianjin First Chemical Reagent Plant (Tianjin, China). Dodecanol was purchased from Shanghai Chemical Reagents Co. of the Chinese Medicine Group (Shanghai, China). Anhydrous sodium acetate, anhydrous sodium carbonate, and sodium bisulfite were from Chenfu Chemical Reagent Plant (Tianjin, China). Triethylamine, potassium persulfate (KPS), petroleum ether, acetic ester, and anhydrous ethanol were purchased from Fu Yu Fine Chemical Co., Ltd. (Tianjin, China). Chlorine alkene was provided by Yueyang Chemical Plant of Baling Petrochemical Co. (Yueyang, Hunan, China). Acetone was acquired from Da-Mao Chemical Reagent Plant (Tianjin, China). Formic acid was purchased from Tianjin Chemical Reagent Co., Ltd. (Tianjin, China). MA and BA were purchased from Wulian Chemical Plant (Shanghai, China). *n*-Pentanol was obtained from Shanghai Fourth Reagent Plant (Shanghai, China). Sodium chloride (NaCl) was purchased from

Yueqiao Reagent and Plastic Co., Ltd. (Guangdong, China). The home-made reactive surfactant SAA was purified by column chromatography; water was purified by deionization and subsequent distillation in an all-glass apparatus.

Synthesis and characterization of the reactive surfactant SAA

SAA was synthesized with the sequence of reactions shown in Scheme 1. ¹H-NMR spectra were obtained with a Varian Inova 400 instrument, and IR spectra (Varian Co. Ltd., USA) were recorded on a WQF-410FT instrument (KBr pellet) (Beijing Beifenruili Analytical Instrument (Group) Co. Ltd., China).

Maleic dodecanol monoester (MDM)

Maleic anhydride (0.21 mol), dodecanol (0.20 mol), and anhydrous sodium acetate (0.20 g) were placed in a round-bottom, four-necked flask equipped with a stirring bar, a condenser, and a thermometer. The contents were heated up 90°C in 10 min and stirred for 3 h, and then the crude monoester (MDM) was obtained; it could be used directly in further synthesis. To determine its structure, the crude MDM was crystallized three times from acetone, and colorless MDM crystals were obtained (75% yield).

¹H-NMR (400 MHz, CDCl₃, δ): 0.88 (t, *J* = 6.8 Hz, 3H, CH₃), 1.26 [brs, 16H, (CH₂)₈], 1.30 (m, 2H, CH₃CH₂), 1.73 (m, 2H, OCH₂CH₂), 4.29 (t, *J* = 6.8 Hz, 2H, OCH₂), 6.38 (d, *J* = 12.8 Hz, 1H, CHCHCOOH), 6.49 (d, *J* = 12.8 Hz, 1H, CHCHCOOH).

Maleic dodecanol allyl diester (MDA)

Anhydrous sodium carbonate (0.20 mol) was added to the aforementioned crude monoester (MDM), and the contents were heated for 30 min between 75 and 80°C; after the reaction mixture cooled between 50

and 60°C, chlorine alkene (40 mL), acetone (50 mL), and triethylamine (10 mL) were added, and the mixture was stirred for 6 h. After filtration, rotary evaporation, washing, and drying with anhydrous Na₂SO₄, crude MDA was obtained; it could be used directly in further synthesis. To determine its structure, the resulting crude MDA was subjected to column chromatography on silica gel (petroleum ether/ethyl acetate = 10:1) to afford the pure compound MDA as a transparent and colorless liquid (60% yield).

¹H-NMR (400 MHz, CDCl₃, δ): 0.88 (t, *J* = 6.8 Hz, 3H, CH₃), 1.26 [brs, 16H, (CH₂)₈], 1.30 (m, 2H, CH₃CH₂), 1.66 (m, 2H, OCH₂CH₂), 4.18 (t, *J* = 6.8 Hz, 2H, OCH₂), 4.69 (d, 2H, *J* = 6.0 Hz, CHCH₂), 5.26–5.39 (m, 2H, CH₂), 5.90–6.00 (m, 1H, CHCH₂), 6.26 (s, 2H, CHCH).

SAA

A sodium bisulfite (0.053 mol) solution (mass fraction = 40%) was dropped into the aforementioned crude MDA (0.05 mol) for 1 h at 110°C, and the contents were heated to 120°C and stirred for 3 h; crude SAA was obtained. To determine its structure, the resulting crude SAA was subjected to column chromatography on silica gel (petroleum ether/ethyl acetate = 3:1) to afford the pure compound SAA as a light yellow, gelatinous solid (65% yield).

¹H-NMR (400 MHz, CDCl₃, δ): 0.88 (t, *J* = 6.8 Hz, 3H, CH₃), 1.25 [brs, 16H, (CH₂)₈], 1.30 (m, 2H, CH₃CH₂), 1.58 (brm, 2H, OCH₂CH₂), 1.71 (s, 3H, =CCH₃), 3.19 (m, 2H, CH₂CO₂), 4.01–4.17 (brd, 2H, OCH₂), 4.34 (m, 1H, CHSO₃Na), 4.55–4.69 (brd, 2H, CHCH₂), 5.19 (d, *J* = 9.2 Hz, 1H, CH₂), 5.31 (t, *J* = 17.2 Hz, 1H, CH₂), 5.82–5.92 (brm, 1H, CH). IR (KBr, ν, cm⁻¹): 2925, 2854, 1738, 1647, 1464, 1221, 1165, 1051, 993, 926, 723.

Pseudoternary phase diagrams

The reactive surfactant SAA and *n*-pentanol were mixed according to different mass ratios (*k* = mass of SAA/mass of *n*-pentanol) to form one component as an emulsifier; MA and BA were mixed according to the mass ratio needed to form an oil phase (mass of MA/mass of BA = 3 : 7). The aforementioned emulsifier and oil phase were mixed in different proportions (the mass ratio of the emulsifier to the oil phase was designated *R*) and were put in a ground tube with 20 mL to blend; the ground tube was then placed in a constant-temperature implement to produce a temperature of 25 ± 0.1°C. A water phase was dripped into the two components by a water dilution method, and then the phase transformation points in the system were observed with the naked eye. The first phase transformation

point occurred when the system varied from feculence to limpidity, the second phase transformation point occurred when the system varied from limpidity to feculence, the third phase transformation point occurred when the system varied from feculence to limpidity again, and the fourth phase transformation point occurred when the system varied from limpidity to feculence again. The temperature was kept constant for about 10 min in the vicinity of every phase transformation point, and then the phase transformation point was determined after the phase remained stable and balanced. Finally, the mass proportions of the emulsifier, oil phase, and water were calculated at the phase transformation points, and pseudoternary phase diagrams were presented.

Microemulsion polymerization

Specimens were confected through the choice of three different points in a single-phase realm [A, B, and C in Fig. 1(b)] with the initiator KPS. Each specimen and 0.02 g of KPS were mixed and then put into a 25-mL compression-resistance hermetical tube. Systems were heated to an appropriate temperature in aqueous holloware so that the polymerization reaction could be carried out. There was some white filaceous matter at about 10 to 15 min, and a lot of white solid latexes were made by polymerization in 1 h. The polymer was deposited with ethanol, whereas some excessive reactive surfactant and small molecule impurities on the polymer were eliminated with ethanol. Solid latexes were dried for 24 h at 60°C and were sprayed to be observed with scanning electron microscopy (SEM). The glass-transition temperature was measured with a differential thermal analyzer; the scope of the measured temperatures was -80 to 60°C, and the calefactive velocity was 10°C/min.

RESULTS AND DISCUSSION

Influence of the cosurfactant on the microemulsion

The influence of the cosurfactant (*n*-pentanol) on the microemulsion phase diagrams was examined separately at *k* values of 2 : 1, 1.5 : 1, 1 : 1, and 1 : 2. The diagrams in Figure 1(a–d) correspond to the phase behaviors of the microemulsion systems with different *k* values.

The variation of the microemulsion area with the *k* value actually reflects the influence of the *n*-pentanol content on the formation of the microemulsion. As shown in Figure 1, when the gross of the emulsifier was fixed, the microemulsion area gradually diminished with *n*-pentanol increasing. It was very difficult to produce a phase transformation point and form a microemulsion when the *k* value was up to

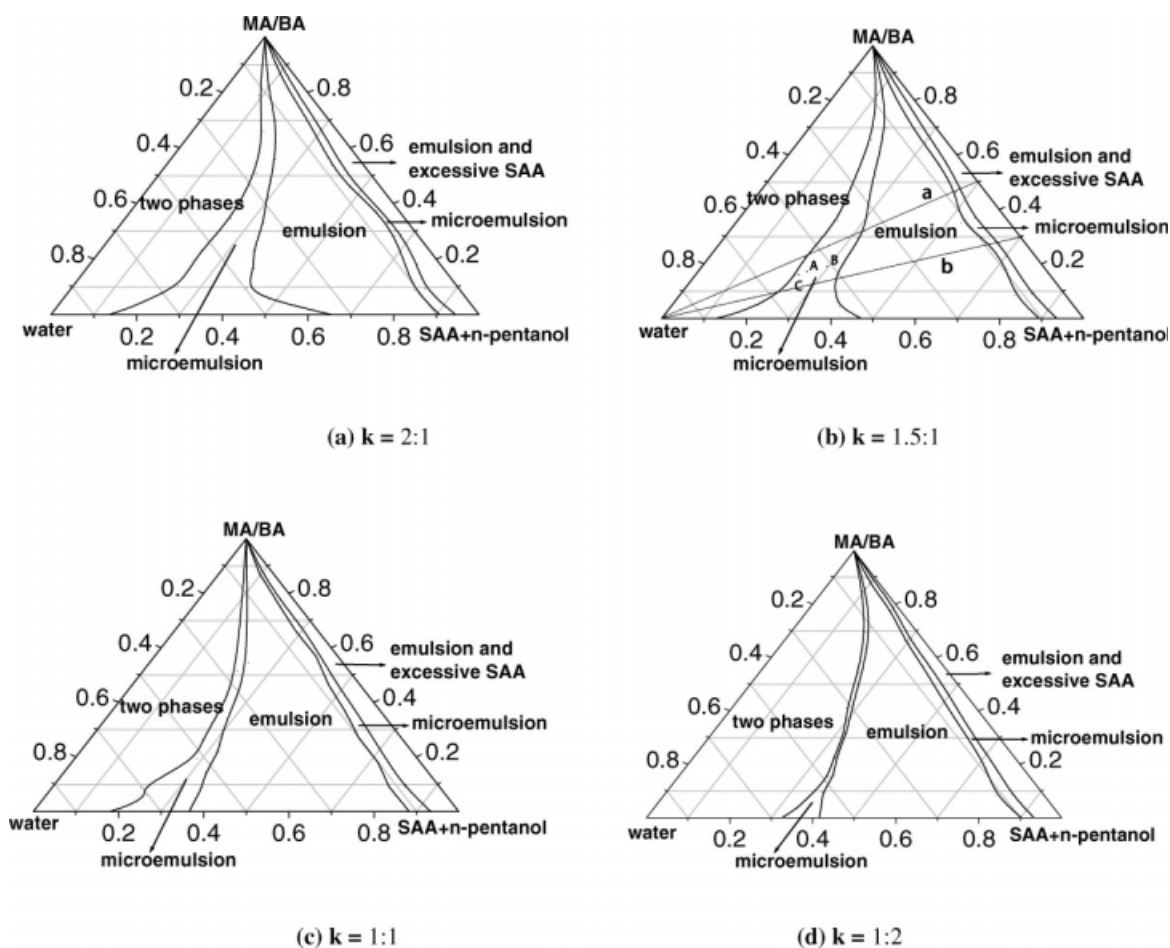


Figure 1 Pseudoternary phase diagrams of SAA, *n*-pentanol, MA/BA, and water.

1 : 3. This was because the influence of the *n*-pentanol content on the interfacial film of the micella formed by SAA was small and not evident. With the *n*-pentanol content increasing, the solubilization of *n*-pentanol in the micellar barrier layer formed by SAA increased, so the flexible performance of the mixed interfacial film formed jointly by the surfactant and *n*-pentanol was enhanced greatly.¹⁶ In addition, *n*-pentanol was also able to destroy the floeberg structure of water surrounding the mixed interfacial film¹⁷ and accordingly improved the flexible performance of the mixed interfacial film. However, when the *n*-pentanol content was excessive, it could, to some extent, dissolve in both the water phase and the oil phase and could associate with the polar group of the surfactant molecule, making the film loose. Furthermore, an excess of *n*-pentanol could reduce the intensity of the film and the stability of the microemulsion, making the microemulsion area smaller. In addition, the price of the reactive surfactant was very high, and the content could not be too high, so it was better to use a *k* value of 1.5 : 1 to prepare the microemulsion.

Influence of the electrolyte on the microemulsion

Figure 2 shows phase diagrams of a microemulsion added to NaCl whose mass concentration was 0.5% when the *k* value was 1.5 : 1. As shown in Figure 2, the area of the microemulsion was a bit reduced when it was added to the salt electrolyte, but the influence was not too great. This may be the reason

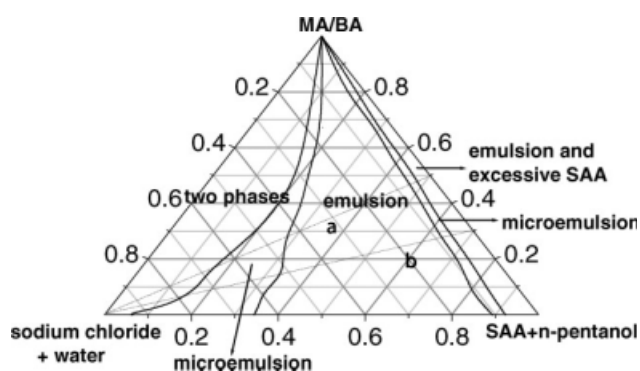


Figure 2 Pseudoternary phase diagram of SAA, *n*-pentanol, MA/BA, and NaCl.

that the counterion may compress the diffuse double layer and decrease the hydrophilicity of the ionic surfactant.¹⁸

Conductivity

Figure 3 shows the conductivity curves of the SAA/*n*-pentanol/MA/BA/water pseudoternary system by the water dilution method. Along the routes including $R = 5 : 5$ [a line in Fig. 1(b)], the conductivity increased slowly with the water content increasing, and the system could not form a conducting chain when the mass proportion of water was below 34.6%, so this area was a water-in-oil (W/O) microemulsion under the condition of $R = 5 : 5$. When the mass proportion of water was between 34.6 and 54.3%, a conducting chain was formed; the conductivity increased rapidly with the water content increasing, and a percolation phenomenon appeared,¹⁶ so the system formed a bicontinuous (BC) structure. When the mass proportion of water was above 54.3%, the concentration of conducting ions achieved its maximum, and the conductivity reached its maximum. When the water content increased again, the conductivity was dominated by water and decreased with the water content increasing, so the system was an oil-in-water (O/W) microemulsion. In the same, under the condition of $R = 7:3$, the system was a W/O microemulsion when the mass proportion of water was below 50.2%, the system formed a BC when the mass proportion of water was between 50.2 and 65.2%, and the system was an O/W microemulsion when the mass proportion of water was above 65.2%.

The conductivity of the SAA/*n*-pentanol/MA/BA/brine pseudoternary system was determined by the water dilution method, and the conductivity curves are shown in Figure 4. Along two routes

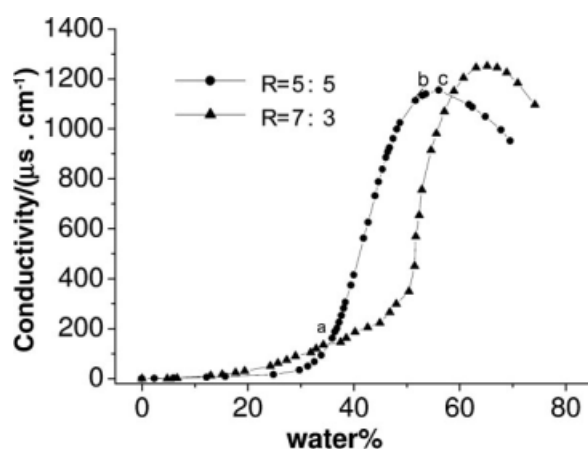


Figure 3 Relationship between the conductivity and volume of water in an SAA/*n*-pentanol/MA/BA/water system.

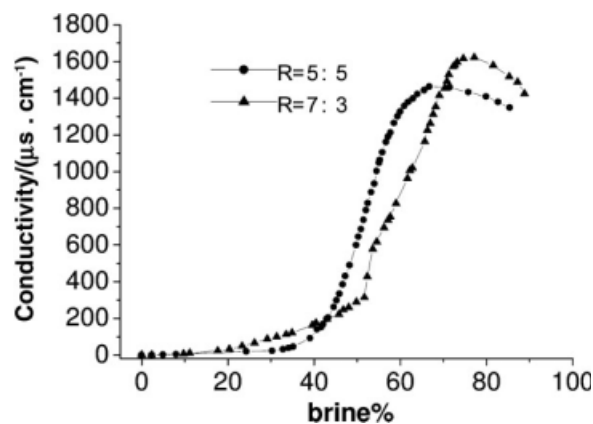


Figure 4 Relationship between the conductivity and volume of a NaCl solution in an SAA/*n*-pentanol/MA/BA/brine system.

including $R = 5:5$ and $R = 7:3$ (directions a and b in Fig. 2), the addition of the electrolyte could enhance the conductivity of the system, but the partition of the microemulsion area in the brine system was not distinct from that in the water system, and this was in accordance with the aforementioned phase diagrams.

Microemulsion polymerization

IR spectroscopy analysis

When the temperature was 80°C, the mass proportion of the emulsifier including SAA and *n*-pentanol was 25.79%, the mass proportion of the monomer including MA and BA was 17.19% [point A in Fig. 1(b)], and the mass proportion of the water was 57.02%. Samples for IR spectra were washed with ethanol to removal small molecule impurities and then dried *in vacuo* to form films. IR spectra were recorded with a Vector 33 instrument (Bruker Co., Germany).

In the Fourier transform infrared (FTIR) spectrum of acrylate latex (Fig. 5), the peaks at 3556 and 3450 cm^{-1} are related to the frequency doubling band of the asymmetrical and symmetrical stretching vibrations of the carbon-oxygen double band,

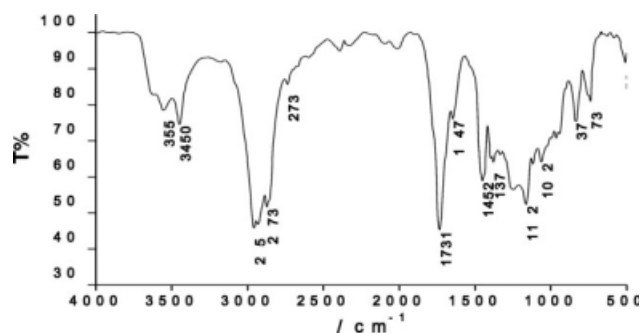


Figure 5 FTIR spectrum of acrylate latex.

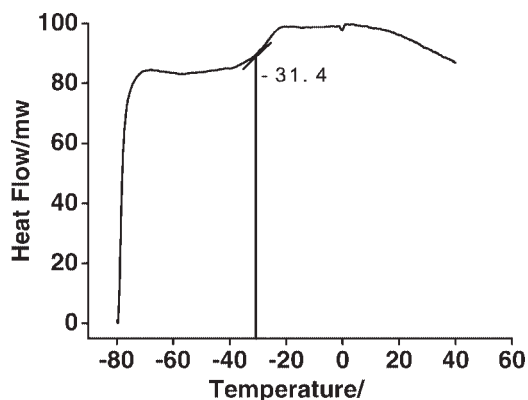


Figure 6 DSC of acrylate latex.

respectively; the peaks at 2958 and 2873 cm^{-1} are related to the stretching vibration band of the carbon–hydrogen bond on methyl and methylene. The peaks at 1452 and 1378 cm^{-1} are related to the in-plane and out-of-plane bending vibration bands of the carbon–hydrogen bond on methyl and methylene, respectively, and the peaks at 1245 and 1163 cm^{-1} are related to the vibration band of the carbon–oxygen–carbon band on the ester group. The peak at 1062 cm^{-1} is related to the characteristic absorption band of the carbon–sulfur band. The peak at 837 cm^{-1} is related to the stretching vibration band of the carbon–oxygen double band on the BA group, and the peak at 738 cm^{-1} is related to the deformation vibration band of long methylene. The peak at 1731 cm^{-1} is related to the stretching vibration band of the carbon–oxygen double band, and the peak at 1647 cm^{-1} is related to the stretching vibration band of the carbon–carbon double band; its intensity is very feeble, showing that little remained of the carbon–carbon double band and that almost all the monomers were used in the copolymerization. In addition, the reactive surfactant SAA could to some extent participate in the polymerization with the monomers.

Differential scanning calorimetry (DSC) analysis

When the temperature was 80°C , the mass proportion of the emulsifier, including SAA and *n*-pentanol, was 25.79% ; the mass proportion of the monomer, including MA and BA, was 17.19% [point A in Fig. 1(b)]; and the mass proportion of the water was 57.02% . The DSC figure of the acrylate latex is shown in Figure 6. The glass-transition temperature was measured with a PerkinElmer DSC7 instrument (test conditions: a temperature range of -80 to 60°C and a heating rate of $10^\circ\text{C}/\text{min}$).

As shown in Figure 6, the polymer latex film had only one glass-transition interval, and its glass-transition temperature was about -31.4°C . That was on the transition at the glass-transition temperatures of the homopolymers of poly(methyl acrylate) and poly(butyl acrylate), and this suggested that there were no corresponding homopolymers and that there was good copolymerization. However, the actual glass-transition temperature was -38.47°C and was higher than the calculated value; maybe this occurred because the anionic reactive surfactant participated in the copolymerization and made the glass-transition temperature increase.¹⁹

Surface structure analysis

The polymer latex was dried for 24 h at 60°C , and then the obtained solid polymer latex was sprayed with gold for observation with a JSM-25S scanning electron microscope (JEOL Co., Japan). Figure 7 shows the SEM micrographs of polymer latexes at different temperatures with the same formula [point A in Fig. 1(b)]. As shown in Figure 7, the surface of the polymer latex was more sequential and regular when the polymerization temperature was lower. When the polymerization temperature reached 90°C , the surface structure of the polymer latex was destroyed severely because too high a temperature destroyed the microemulsion structure and distorted the interfacial film to some extent.²⁰

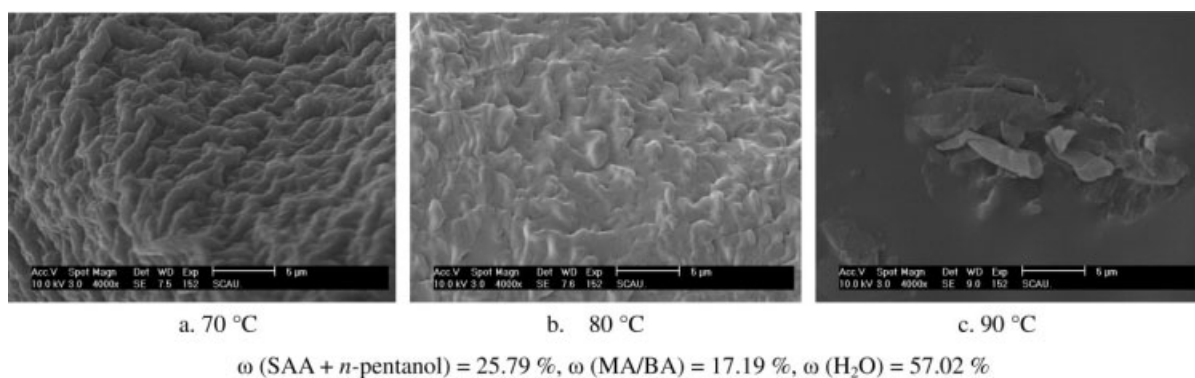


Figure 7 SEM micrographs of polymer latexes at different temperatures (mass proportion of SAA and *n*-pentanol = 25.79% , mass proportion of MA/BA = 17.19% , mass proportion of H_2O = 57.02%).

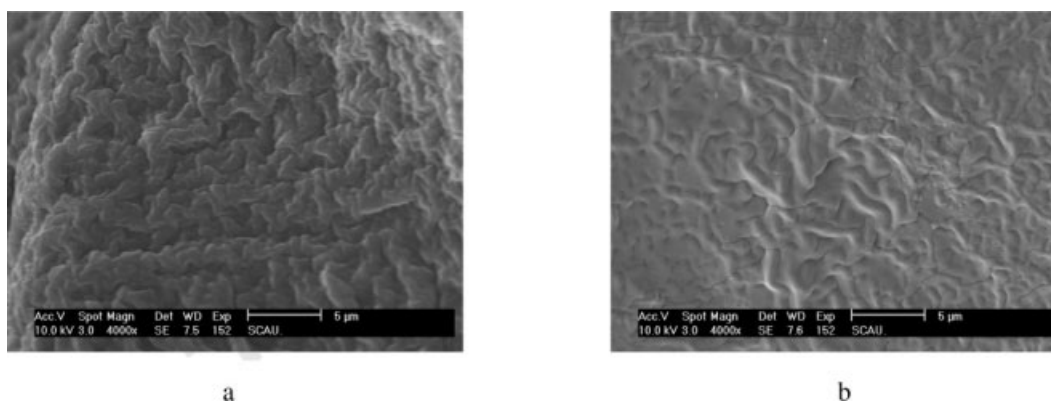


Figure 8 SEM micrographs of polymer latexes with different formulas: (a) mass proportion of SAA and *n*-pentanol = 28.90%, mass proportion of MA/BA = 19.27%, and mass proportion of H₂O = 51.83% and (b) mass proportion of SAA and *n*-pentanol = 23.35%, mass proportion of MA/BA = 15.57%, and mass proportion of H₂O = 61.08%.

Figure 8 shows SEM micrographs of polymer latexes with different microemulsion formulas at 80°C. The formula of Figure 8(a) is point B in Figure 1(b), and the formula of Figure 8(b) is point C in Figure 1(b). Contrasting Figure 8(a,b) with Figure 7(b), we know that the polymer latex was transformed gradually from an open porous structure to a closed porous structure when its pregnant microemulsion varied from a BC structure to an O/W structure.

CONCLUSIONS

Pseudoternary phase diagrams of quaternary microemulsion systems composed of the reactive surfactant SAA, *n*-pentanol, MA/BA, and water were examined. When the mass ratio of SAA to *n*-pentanol was 1.5:1, the prepared microemulsion was optimal.

The microemulsion area was a bit reduced when the NaCl electrolyte was added, but the influence was not too great.

A conductance technique suggested that there were three structures in the microemulsion system: W/O, O/W, and BC.

In the microemulsion polymerization, the reactive surfactant SAA could participate with the monomers to some extent; the glass-transition temperature of the latex was -31.4°C. The polymer latex was transformed gradually from an open porous structure to a closed porous structure when its pregnant microemulsion varied from a BC structure to an O/W structure.

References

- Hu, A. X.; Chen, X. W.; Yao, Z. G. *Fine Chem* 2006, 23, 234.
- Gan, L. M.; Chew, C. H. *Colloid Surf A* 1997, 123, 681.
- Hentze, H. P.; Kaler, E. W. *Curr Opin Colloid Interface Sci* 2003, 8, 164.
- Zhang, Y.; Fang, Y.; Lin, S. Y. *Acta Physico-Chim Sin* 2004, 20, 897.
- Zhao, Y. N.; Chen, X. M.; Li, X. H.; Wang, Y.; Wang, C. Y.; Li, M.; Mai, Z. H. *Chem J Chin Univ* 2003, 24, 986.
- Teng, F.; Tian, Z. H.; Xiong, G. X.; Xu, Z. S. *Catal Today* 2004, 93, 651.
- Song, S. F.; Luan, Y. X.; Lu, F. S. *Chin J Anal Lab* 2006, 25, 59.
- Ohlemacher, A.; Candau, F.; Munch, J. P.; Candau, S. J. *J Polym Sci Part B: Polym Phys* 1996, 34, 2747.
- Gan, L. M.; Liu, J.; Poon, L. P.; Chew, C. H.; Gan, L. H. *Polymer* 1997, 38, 5339.
- Guo, Z. L.; Wang, J. T.; Zhu, H. J. *Acta Polym Sin* 2001, 4, 489.
- Wei, Y. B.; Wu, J.; Wu, S. S.; Zheng, C. R. *Polym Mater Sci Eng* 2005, 21, 141.
- Xia, X.; Yao, Z. G.; Li, X. W.; Liu, J. Q.; Dai, X. Y.; Zhang, L. *Chem World* 2006, 47, 473.
- Gan, L. M.; Chew, C. H.; Lye, I.; Ng, S. C. *Polymer* 1994, 35, 2659.
- Gan, L. M.; Chew, C. H.; Lye, I.; Ng, S. C. *J Polym Sci Part A: Polym Chem* 1995, 33, 1161.
- Chieng, T. H.; Gan, L. M.; Chew, C. H.; Ng, S. C. *Polymer* 1995, 36, 1941.
- Mo, C. S.; Wu, S. H. *J Jiangxi Normal Univ Nat Sci Ed* 2001, 25, 144.
- Zhang, X. G.; Zhang, G. Y.; Wang, H. X.; Zhou, Y. W.; Chen, Z. P. *Fine Chem* 2003, 20, 475.
- Hou, C. J.; Fan, X. H.; Huo, D. Q.; Diao, X. Z.; Dong, L.; Tang, Y. K.; Fan, Y. *Chin J Appl Chem* 2007, 24, 401.
- Luo, H.; Wei, Z. G. *Fine Chem* 1997, 14, 42.
- Xue, M. L.; Yu, Y. L. *Chin J Appl Chem* 2003, 20, 986.